

II Latin American Workshop on Computational Neuroscience
São João del-Rei, MG - Brazil - September, 18-20, 2019



Proceedings of the LAWCN 2019



Universidade Federal
de São João del-Rei



PPGEL
PROGRAMA DE PÓS-GRADUAÇÃO EM ENGENHARIA ELÉTRICA



Assessoria
para Assuntos
Internacionais



INTERNATIONAL BRAIN
RESEARCH ORGANIZATION

Neural network classification, coherence and power spectrum analysis with stress database*

Mateus C. Pedrino, Rafael A. C. Arone, Victor H. B. Tsukahara, and Carlos D. Maciel

University of São Paulo, São Carlos School of Engineering, Electrical and Computer Engineering Department, São Carlos, São Paulo, Brazil
<http://www.eesc.usp.br/portaleesc/en/>

Abstract. Electroencephalography is a popular method for brain waves analysis. Each region of the scalp or brain surface has different contribution accordingly to the task that is being performed. Different sorts of techniques are employed to study connectivity between brain regions, and for this paper, the performance of magnitude-squared coherence will be evaluated along with a power spectrum analysis. Coherence and power spectrum analysis will be conducted upon a stress database, which was collected from two of the authors with an electroencephalogram device developed to acquire, filter, display and export electroencephalogram (EEG) data in real-time from OpenBCI equipment. Stressors used were Stroop and Montreal image tasks, and all of the results generated by signal processing methods with these stressors were discussed and compared to a baseline (EEG section performing actions without stress). Collected data was also used to train an artificial neural network with Multilayer Perceptron for stress level classification with two levels. The developed device showed an excellent performance considering hardware limitations. Experimental results with both stressors allowed the proposed methods to be successfully employed and discussed considering that phenomena such as an increase in theta and beta power and coherence were observed for both stressors, which matches the corresponding bibliography even with hardware limitations. The Multilayer Perceptron allowed 95% and 74% of accuracy using magnitude-squared coherence and power spectrum, respectively, as inputs.

Keywords: Coherence · Power spectrum · Multilayer perceptron · Neural network classification · Brain-computer interface.

1 Introduction

Stress is widely present in our daily lives, and it might compromise both mental and physical health, that is why its comprehension is important [46]. Electroencephalography (EEG) along with signal processing tools is an applied method

* Supported by São Paulo Research Foundation (FAPESP) and National Council for Scientific and Technological Development (CNPq).

Stress coherence, spectrum and classification

to help the understanding of human emotional responses such as stress [16]. The power spectrum, connectivity measures and artificial neural networks (ANN) are examples of tools that have been recently applied to EEG stress analysis [3,41]. The standard analysis of EEG data in signal processing uses second-order statistics, the second moment and second central moment [36]. From them, by the use of Fourier Transform, power spectrum (by the Wiener–Khinchin theorem [14]) and the cross-spectrum (when the correlation between signals in the frequency domain is desired) can be calculated [23]. EEG is a method that allows the measurement of scalp conductance through electrodes positioned on the head [52]. These signals are generated from activities of different brain areas, and these signals, along with a frequency domain analysis, allow us to understand the brain state [27].

The study of how different brain regions interact and how this interaction behaves during the execution of specific tasks has been of great interest, for that, connectivity signal processing tools, such as coherence, are used [53]. Coherence can show us if there is a similar or under synchronism activities from different brain areas [47]. High connectivity values indicate a strong interaction among these areas and low values indicate a possible independence [8]. Coherence has also been used to verify brain areas connectivity variation in response to psychological disorders or emotional states such as stress [35]. ANN has been used to classify biomedical datasets [51,6,32]. A possible EEG classification method is Multilayer Perceptron (MLP), which uses supervised learning and cross-validation methods to avoid over and underfitting [25]. For this kind of classification, data has to be preprocessed using filtering methods, Fourier transforms and adequate windows in order to highlight main lobes of interest [26,54,55]. MLP specifically has been used for stress recognition and classification with great performance, that is over 95% of accuracy [1].

This work will explore the analysis and discussions around the application, limitations and behaviour of the power spectrum and magnitude-squared coherence (MSC) applied to EEG signals. The same goal is proposed for the application of classification with MLP to EEG signals. To perform these discussions and study these tools behaviour during a psychophysiological stimuli, Montreal image task [15] and Stroop test [50] were used as stressors during the EEG acquisition. These proposed analyses were motivated by the fact that many times, these tools are used as black boxes and for this reason might conduct to spurious results. That is why their comprehension is so essential even because they are widely applied to biomedical studies [3,35,1]. In order to perform these tasks, an interface connected to the EEG device had to be developed to acquire, filter, display and export EEG data in real-time from a simple EEG acquisition hardware from OpenBCI. The proposed tools will be discussed considering the hardware limitations. Section 2 is going to introduce the theory related to electroencephalography, coherence, power spectrum techniques and MLP. Section 3 presents the interface development and applied methodology. Section 4 reports the results and discussions achieved. To close the paper, Section 5 presents a conclusion.

M. C. Pedrino et al.

2 Theory

This section presents a brief review of the required theory for this paper. Electroencephalography, coherence, power spectrum techniques and MLP are defined. Some equations are established to uniform mathematical notation.

2.1 Electroencephalography Signals

The electroencephalograph is a device that allows brain activity measurement through electrodes on the scalp, and it is a method with great temporal resolution [52].

EEG signals are divided into frequency bands, each one indicating determined conditions of the subject from neuron activity and intrinsic oscillations according to membrane's properties [52]. The first band is delta, which is composed of frequencies lower than 4 Hz, and it appears mainly during deep sleep and diseases that provoke a lack of consciousness [18]. The second band is theta (4 to 7 Hz), which indicates that the subject is doing a repetitive action, under stress, alert or attention [43] and these waves can be acquired at the frontal lobe [42]. Alpha band (8 to 13 Hz) indicates relaxation when awake [44]. Finally, beta waves (13 to 30 Hz) are associated with high stress, logical thinking and problem-solving [39].

The brain is divided into regions that indicate different kinds of activities. These regions are frontal, temporal, parental and occipital lobes. The frontal lobe is responsible by speech and motor activities, while the temporal lobe is responsible by speech processing and memory, the parental lobe is the brain processing area, and for least, the occipital lobe is responsible by eye image processing [52]. The activity of these areas can be measured by electroencephalogram using the 10/20 placement system [31]. It is essential to highlight that EEG signals are commonly affected by noises, especially eye blinking, muscular movements, respiration and heart beating and eye blinking specifically has a general effect over the whole EEG spectrum [22].

2.2 Spectral Estimation

The power spectrum is a measure of power distribution at each frequency of the signal and, for this calculation, Wiener-Khinchin method [14] is used, which is the Fourier Transform of the signal autocorrelation function [14]. However, the method is only allowed to stationary signals, and it is necessary to have a large number of samples, which is not available in most applications [29]. A solution is the use of spectral estimation methods, which considers that the signal is stationary in a determined time interval, allowing the power distribution calculus [9].

One of these spectral estimation methods is Welch Periodogram. The result of the Welch Periodogram is the mean of smaller samples power spectrum, decreasing the variance of the estimation [57]. The selection of each sample is made by the use of windows functions, and one of these is the prolate spheroidal

Stress coherence, spectrum and classification

window, which is an optimal window that has the maximum energy at the main lobe [34]. Once the power spectral density of a signal ($S_{xx}(e^{2j\pi f})$) is already estimated with sampling frequency F_s and N number of points, the average power within a band (limited by f_1 and f_2) can be determined from Eq. (1) [49].

$$P(e^{j2\pi f_1}, e^{j2\pi f_2}) = \frac{F_s}{N} \sum_{k=f_1}^{f_2} S_{XX}(e^{j2\pi k}) \quad (1)$$

Welch periodogram is commonly used for power spectral density because of its excellent performance with noise compared to traditional periodogram and Bartellet methods, although with worse spectral resolution [36].

Another spectral estimation method is by the use of time-frequency transforms, as Short Time Fourier Transform (STFT), which allows Fourier Transform to be applied to non-stationary signals, dividing the signal into smaller parts and calculating the Fourier Transform of each part [2]. It generates a spectral analysis of each time interval, giving when each frequency is showed [45]. The results of this methods depend on the length of the window (L), and the size of sliding window shift (D) and they are linked to the spectral and temporal resolutions of the data [12]. The expression of the STFT can be seen below, with $f_m = \frac{m}{L}$ and $t_n = nD$:

$$X(t_n, f_m) = \sum_{k=0}^{L-1} x(k)w(nD - k)e^{-j2\pi \frac{m}{L}} \quad (2)$$

The result of the STFT has a tradeoff between the variance of signal time and frequency. This relationship is expressed by the fact that the product between time and frequency standard deviations is constant, showing that the deviations are inversely proportional, which is called the uncertainty principle [13]. Thus, although it is not possible to have all frequencies that occur at a determined instant, it is possible to determine the power in a range of frequencies within a time interval.

2.3 Coherence

Coherence can be seen as a linearity measurement between two signals [10], and this kind of function applies to a great sort of purposes, such as system identification, signal-to-noise ratio (SNR) and time delay measurements [11]. Mathematically coherence can be defined as a complex coherence, which is the ratio between the cross-spectrum of two signals ($S_{xy}(e^{2j\pi f})$) and the root of the product between each signal power spectrum ($S_{xx}(e^{2j\pi f})$ and $S_{yy}(e^{2j\pi f})$), or a magnitude-squared coherence (MSC or $C_{xy}(e^{2j\pi f})$), which is the squared complex coherence [11], expressed at Eq. 3. It is important to highlight the cross-spectrum returns a cross-correlation between signals in the frequency domain [36].

M. C. Pedrino et al.

$$C_{xy}(e^{j2\pi f}) = \frac{S_{xy}^2(e^{j2\pi f})}{S_{xx}(e^{j2\pi f})S_{yy}(e^{2j\pi f})} \quad (3)$$

MSC as expressed at Eq. 3 is frequency-dependent and returns a normalized value between 0 and 1. Value 1 happens in two main situations: when signals are represented by a single sample set (which does not have any physical meaning) and when there is no amplitude e phase variation between two signals across time for a given frequency component once phase and amplitude variation are able to change coherence [10]. Also, MSC can be applied to EEG signals to verify coupling between brain regions [33] and high MSC values might be seen as a functional or structural connection between cortex regions from which the signals were acquired [17].

2.4 Data Classification

The use of artificial neural networks (ANN) to solve pattern classification problems is a widespread method [37]. Among these methods, it is highlighted the architecture which uses supervised learning, which needs a data set with the labelled input and desired output of each sample to perform classification [24]. A typical structure that allows these classifications with generalization is the Multilayer Perceptron. This method is composed of smaller structures called Perceptrons, which uses non-linear models to make a linear classification [19]. The arrangement of these smaller parts is made by the organization in layers without feedback. Layers are divided into input, hidden and output, and the signal direction is always from the input to the output. This division allows the non-linear classification of the data [20].

The training is made by *backpropagation* algorithm [24], which adapts the weight w of each input in each neuron. This adaptation is dependent on the difference between the actual model output and the desired output for each input data set [19]. The resulting value is multiplied by the input sample and learning rate (defined previously), and it is added to the actual weight value. This algorithm runs until the difference between two consecutive weights are smaller than a threshold [24].

3 Materials and Methods

In this section, information about the developed EEG interface is reported, as well as the applied methodology, including algorithms and the computational environment.

3.1 Materials

An interface was developed to acquire, filter, display and export data from EEG source Ultracortex “Mark IV” EEG Headset made by OpenBCI. After the acquisition, the Cyton board converts the analogical signal to digital with a sampling

Stress coherence, spectrum and classification

rate of 250 Hz and communicates via Bluetooth with a dongle, which sends the data to the computer. The components of the used hardware can be seen in Figure 1. The computational environment to develop and run the developed software was Ubuntu 16.04 in a Dell Vostro 5470 (Intel Core i5 and 8GB RAM) using Python 3.5.2 as the programming language.

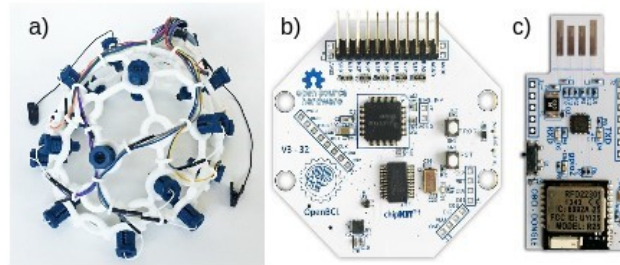


Fig. 1: a) Ultracortex ‘Mark IV’ EEG Headset hardware with 8 electrodes and 10/20 system possible positions. b) Cyton Board with 250Hz of sampling rate. c) Dongle that communicates via Bluetooth with Cyton board.

3.2 Interface development

The developed interface basic functioning can be represented by the Figure 2.

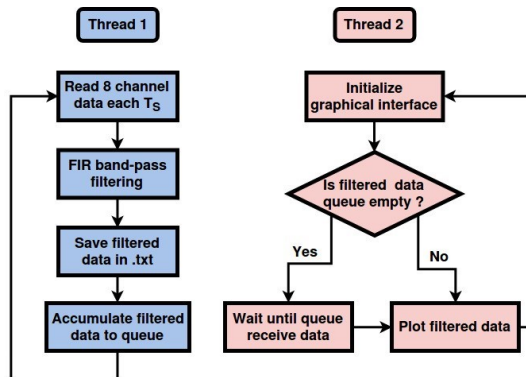


Fig. 2: Interface operating scheme for EEG acquisition, filter and display in real-time using multithreading.

For band-pass FIR filtering, 5Hz and 50Hz were used as cutoff frequencies with Hann window [36]. It is important to highlight that 5Hz was used as low

M. C. Pedrino et al.

cutoff frequencies in order to decrease the DC level influence significantly and there is no problem about it once delta band is not used to the proposed analysis. Moreover, 50Hz was used to lower the influence of the electrical system, which in the laboratory was 60Hz.

3.3 Tests description

With the developed software, Stroop and Montreal image tasks [15,50] were performed with two of the researchers, and the results were compared to regular activity with the same researchers. Stroop test consists of inducing a conflict produced by reading and colour perception. The objective of this test is to speak the name of the text colour, which is different from the text word itself [50]. For instance, the word yellow is coloured in blue, so the right answer after seeing the word picture is blue. The other task (Montreal Imaging Stress Task) consists of performing mental calculus (without any calculating tool) with a limited time, and the level is gradually increased, starting with sum and subtraction of two numbers with only one digit, until achieving operations with four numbers using both multiplication and division with numbers in range from 0 to 100, and also the time is decreased inasmuch as the user gets the right answer. Both tasks were implemented in Python and appended to a new thread along with the former interface threads (Figure 2), so the subject can perform Stroop and Montreal Image tasks while the software acquires, filters, displays and exports the EEG data. Stroop and Montreal image tasks were chosen based on the existing correlation between them and the stress effect on EEG power spectrum [15,21].

Electrodes positions for each channel were : FP2 (Ch0), FPz (Ch1), F8 (Ch2), Cz (Ch3), F4 (Ch4), P3 (Ch5), T6 (Ch6) and T4 (Ch7). These positions were chosen considering areas with great stress sensitivity used in previous works and bibliography [4,5,56]. Once EEG is already collected, before applying power spectrum and MSC to each channel data with both stressors and compare with normal EEG activity, a convenient temporal interval had to be selected. This had to be done once the available hardware did not include electrooculography (EOG) and, therefore, the blinking effect was present and capable of disturbing the analysis. In order to solve this issue, intervals without many blinking peaks were chosen for power spectrum and coherence analysis.

3.4 Applied methodology

Average power in each band (theta, alpha and beta) was determined from the power spectrum estimated with Welch's periodogram using Eq. (1) and MSC coherence was computed with a generalization of Welch's periodogram in order to estimate cross-spectrum [57]. Both power spectrum and MSC were implemented with Python 3 using the last version of *scipy.signal* library [28]. It's important to highlight that the choice for Welch's method was made considering its good performance dealing with noise [36], which is our main concern considering that the acquisition hardware is not good enough for achieving biomedical conclusions

Stress coherence, spectrum and classification

however serves the goal of exploring the performance and discussions around the proposed signal processing and machine learning tools.

For coherence discussion, an average MSC was computed for each pair of electrodes combination, and the ratio between the average MSC during stress manifestation (Montreal and Stroop) and regular activity was computed for theta, alpha and beta bands. These results were generated in a correlogram with the same colour scale in order to compare results more easily. In this colour scale, red represents an increase in average MSC and blue represents a decrease. Also, in the proportion that the colour gets darker, these variations become higher.

For the signal classification discussion, two classifications were made, each one using different kinds of input. The first one used the results from the Short Time Fourier Transform to acquire the power of each band over time with a window containing 256 taps, and the power of each band was normalized considering the total signal power. So, with 8 EEG channels and 3 frequency bands, 24 inputs were generated. The second classification used the mean coherence of all electrodes combinations within each band, with a Slepian window [59] containing 512 taps and 50% of overlap, totalling 168 inputs.

To assign labels to the training set, the task that was being performed during the EEG recording with two of the researchers was considered. Briefly, class “without stress” (or 0) was assigned for signals intervals captured during regular activity, and class “with stress” (or 1) was assigned for signals intervals captured during Stroop or Montreal tasks where the power spectrum and MSC indicated stress manifestation according to the corresponding bibliography [43,42,4,39,3]. The results of each combination were plotted in a graph. For one hidden layer, the graph was the accuracy versus the number of neurons. For two hidden layers, the axes were the number of neurons at each layer, and the accuracy was represented by a colour scale, with darker parts indicating a higher score. The dataset had a total of 249 samples, of these, 53.7% corresponding to the non-stressed state.

The MLP model was implemented using the *scikit-learn* library [38]. The applied MLP topology used sigmoid as an activation function, learning rate of 0.001, and *adam* solver to optimize the weights. This optimization is based mainly in the fact that the learning rate adapts accordingly to the first and second momentum of the gradient [30], where the initial momentum was set to 10^{-5} .

4 Results and discussion

In this section results and discussions around the developed interface to perform the study is reported, as well as the applied methodology, including coherence, power spectrum and MLP.

4.1 EEG interface functioning

The interface developed to connect to the EEG device worked adequately, and the acquisition and display features can be seen in Figure 3.

M. C. Pedrino et al.

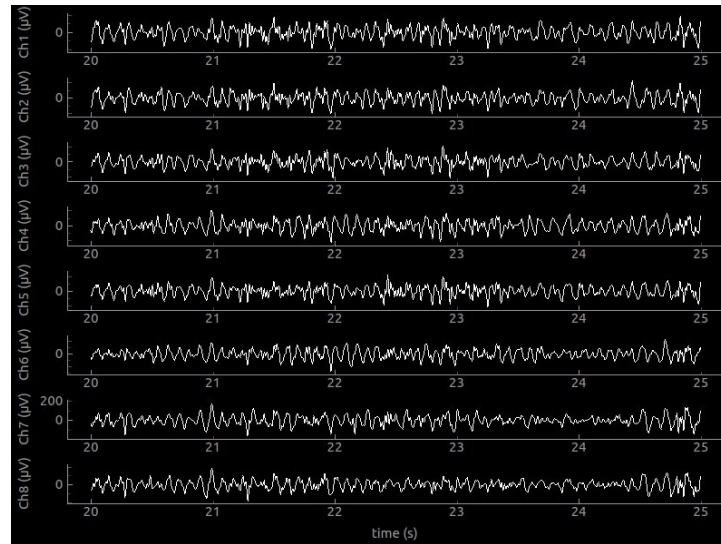


Fig. 3: Developed interface with real-time acquisition, filtering, display and data export working during data collect with 5 seconds of time range.

4.2 Tests results and discussion

The applications developed to perform Stroop and Montreal tasks can be seen in Figure 4. Stroop application generates samples with different words and colours each 5s, although, for visual purposes, some cases were joined in the same figure. Figure 4 shows different difficulty levels got together in the same picture.

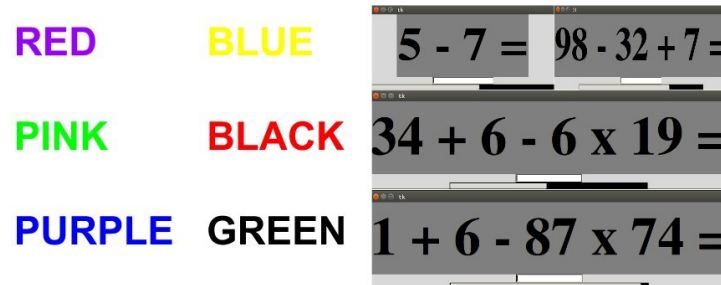


Fig. 4: Several samples of Stroop developed application and different difficulty levels of implemented Montreal Image task application.

Choosing intervals of EEG raw data where the blinking effect is almost imperceptible, the following mean power radar plots for each band, each electrode position and each activity were generated.

Stress coherence, spectrum and classification

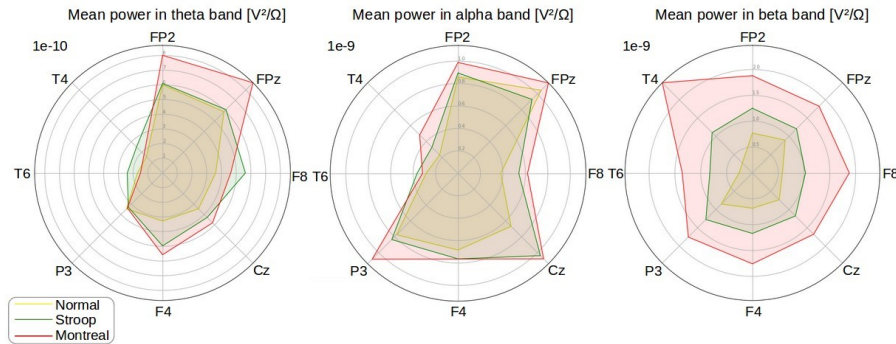


Fig. 5: Mean power in theta, alpha and beta bands for normal activity, Montreal and Stroop tasks.

As can be seen in Figure 5, average power computed in theta, alpha and beta bands through the proposed power spectrum estimation methods could handle the noise present (variance reduction) in the acquisition platform and the signal. These results were consistent once theta band is related to attention and stress tasks, so it's expected that mean power in this band, especially in the frontal regions, increases with stress manifestation (Stroop and Montreal stimuli) [43,42]. Furthermore, beta waves had a huge power increase during stress manifestation especially during Montreal image test which meets the fact that increases in beta power are strongly related to attention and cognition activities, which is true mainly in Montreal image task [4,39].

The blinking effect in different EEG signal intervals for each of the activities proposed can be seen in Figure 6. If we focus on regular activity interval (highest blinking density), the power spectrum consequence of blinking effect at a low sampling rate (250Hz) can also be seen on the right side of Figure 6.

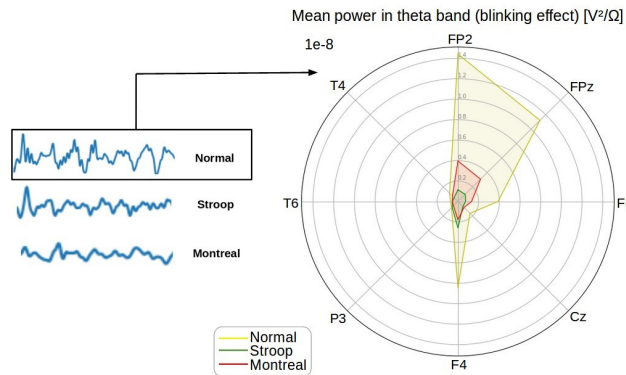


Fig. 6: Blinking effect in selected intervals of EEG collected signals and further power spectrum analysis focused on regular activity interval.

M. C. Pedrino et al.

If blinking peaks were more selective (this means more similar to an impulse) it would not be a problem for spectral analysis once the Fourier transform of an impulse is a DC level in the frequency domain and it could be easily removed before power spectrum and MSC analysis. However, as it can be seen in Figure 6, those peaks are more similar to a square window than to an impulse, and this happens because of the low sampling rate (250Hz), so the frequency domain is affected differently by some function close to a cardinal sine, which sharply increases power density in lower frequencies (theta band) in scalp regions closer to the eyes (frontal region : FP2, FPz and F4).

For coherence analysis, Figures 7 and 8 were generated.

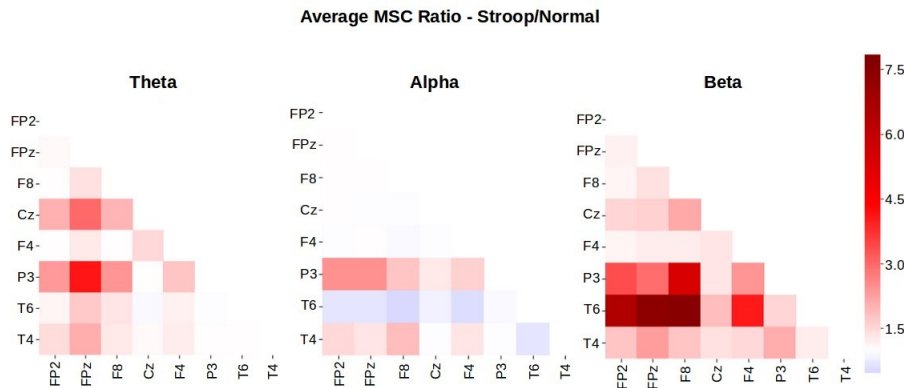


Fig. 7: Average MSC ratios between Stroop task and normal activity signals.

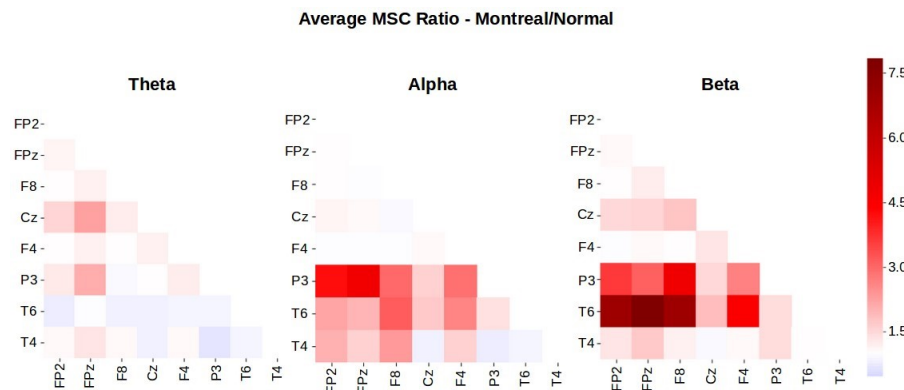


Fig. 8: Average MSC ratios between Montreal task and normal activity signals.

Stress coherence, spectrum and classification

One main characteristic of the MSC is the fact that its value is high (almost one) for adjacent regions, and it decreases in the proportion that the distance between regions increases [48]. From the Figures 7 and 8 it can be inferred that for neighbouring regions (among the electrode placement chosen), such as P3-Cz and Cz-T4, MSC almost did not vary and for distant regions, such as T6-FPz, T6-FP2 and T6-F8 MSC had the most prominent variations. This fact can be seen as a confirmation that [48] proposes, once if MSC is almost one for near regions independently of the task that is being performed during the EEG recording, a change of task, such as a stressor task, won't be able to vary significantly the MSC between close brain regions and the analogous reasoning is also true for distant brain regions.

Moreover, MSC could also generate consistent results for EEG stress signals once it showed some shared characteristics between both stressors : a majority increase in theta and beta coherence and decrease in alpha coherence (mainly for Stroop case), which goes toward the expected effect during stress stimulated by both stressors [3].

The results for the MLP classification with different topologies can be seen in Figure 9. The maximum accuracy of each case, using coherence and power spectrum as inputs with one and two hidden layers, can be seen in Table 1. The highest values of accuracy and how these values vary with the number of neurons in each layer allow us to know what is the best configuration for this MLP.

Table 1: Maximum accuracy and the number of neurons of each hidden layer for the MLPs trained with each type of input.

Input	Num. of hidden layers	Max. score	Neurons 1st layer	Neurons 2nd layer
Power Spectrum	1	74%	108	-
Power Spectrum	2	71%	39	13
Coherence	1	95%	36	-
Coherence	2	94%	168	115

In Figure 9, the accuracy was higher in the network trained with coherence as input, reaching 95%, while those trained with power spectrum had a maximum of 74%.

The previous results indicated that coherence training had higher classification performance in terms of accuracy than with power spectrum inputs. A difference between results was already expected once the number of inputs in each case is widely different (coherence had 168 inputs, while the mean power spectrum had 24 inputs). Coherence inputs might have its better performance attributed to the fact that this function returns a normalized value between zero and one independently of the subject and mental state, while power spectrum might have high variations and hugely discrepant values depending on the subject and on the mental state [7]. Furthermore, the coherence of the EEG data returns a value that corresponds to how each channel varies in relation to an-

M. C. Pedrino et al.

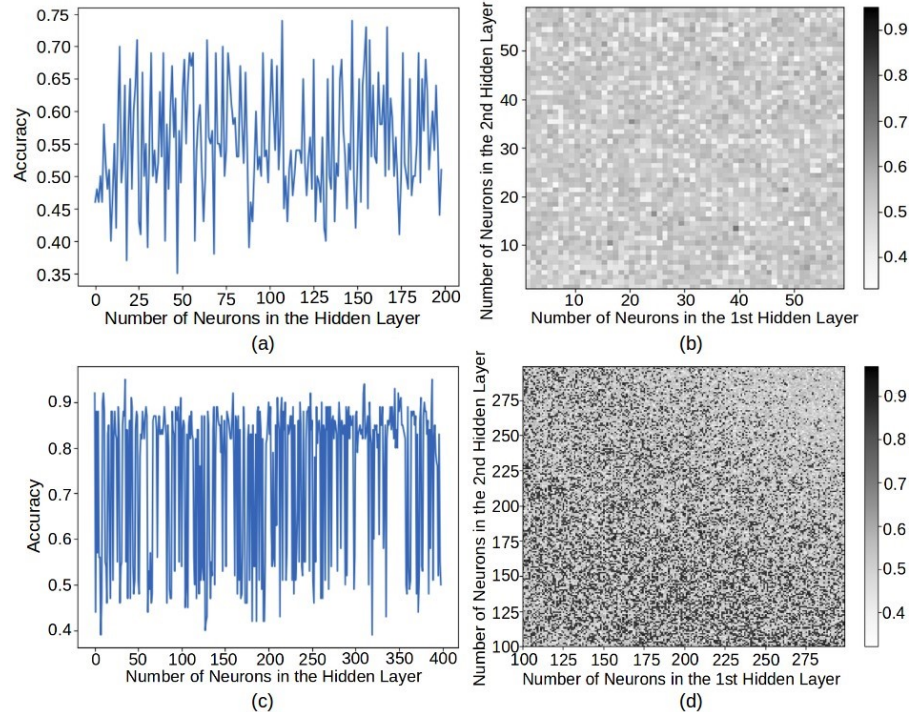


Fig. 9: Neural network accuracy with (a) mean power spectrum as input and one hidden layer, (b) mean power spectrum as input and two hidden layers, (c) mean coherence as input and one hidden layer and (d) mean coherence as input and two hidden layers.

other, in the frequency domain; While the power spectrum analyzes the effect of only one channel each time, which does not imply that functional activity changed, once the functional activity depends on the interaction between different brain regions (as considered by MSC) [40]. Moreover, the approach with the power spectrum as input is more susceptible to the presence of artifacts, mainly in frontal lobes, once power spectrum measures an absolute value, and there is no interaction between channels to compensate the artifact presence [58]. Thus it might be considered the fact that interaction inputs are more discriminant than absolute inputs for MLP stress classification, however, to conclude that, more data with more subjects, better equipment and a study along with medical monitoring is required.

Stress coherence, spectrum and classification

5 Conclusions and recommendations

In a first moment, power spectrum and coherence analysis were able to provide discussions around their applications and background such as noise resistance and blinking effects. These facts were clarified by the contrasting difference in the mean power between regions affected and not affected by eye blinking. Hardware limitations explained how a small sampling frequency could distort an impulse in the time domain and cause an increase in the power spectrum during blinking periods.

EEG power spectrum and MSC variations within intervals without blinking influence observed during the proposed tasks showed behaviours already well established by the corresponding bibliography [43,42,4,39,3] such as an increase in theta and beta band mean power and MSC. These observations showed that even with simple hardware, the software developed to filter and acquire raw data in real time from the EEG source could handle its limitations. Also, a discussion around MSC could provide a relationship between variations observed in MSC and the intrinsic dynamics of this tool when signals from different distant points are tested, that is near regions provided more intense MSC than distant regions [48].

Networks trained with mean coherence presented better scores than with the power spectrum. This fact was observed mainly in the case with one hidden layer, once scores higher than 90% could be achieved. All these conclusions support the fact that for classification purposes, functional activity changes are better expressed by interaction measures (such as MSC) rather than absolute values (power spectrum) as suggested by [40].

For future works, acquisition of more data from a more extensive number of subjects and better acquisition hardware are proposed in order to improve the classification, support the reached results in this paper and verify the statement of the possibility to classify the brain state using coherence. Besides that, tests using other machine learning architectures must be done to verify if they improve the classification performance.

6 Acknowledgements

This study was financed in part by the Research Foundation (FAPESP), grant number: 2017/12213-0, and National Council for Scientific and Technological Development (CNPq), grant number: 2018/14268-6.

References

1. Alić, B., Sejdinović, D., Gurbeta, L., Badnjevic, A.: Classification of stress recognition using artificial neural network. In: 2016 5th Mediterranean Conference on Embedded Computing (MECO). pp. 297–300. IEEE (2016)
2. Allen, J.B., Rabiner, L.R.: A unified approach to short-time fourier analysis and synthesis. Proceedings of the IEEE **65**(11), 1558–1564 (1977)

M. C. Pedrino et al.

3. Alonso, J., Romero, S., Ballester, M., Antonijoen, R., Mañanas, M.: Stress assessment based on eeg univariate features and functional connectivity measures. *Physiological measurement* **36**(7), 1351 (2015)
4. Barlow, D.H.: *Principles and practice of stress management*. Guilford Press (2007)
5. BCN, R.E.L.M.L.: *A Consumer'S Guide to Understanding Qeeg Brain Mapping and Neurofeedback Training*. iUniverse (2018)
6. Benediktsson, J.A., Swain, P.H., Ersoy, O.K.: Neural network approaches versus statistical methods in classification of multisource remote sensing data (1990)
7. Berkhout, J., Walter, D.O.: Temporal stability and individual differences in the human eeg: An analysis of variance of spectral values. *IEEE Transactions on Biomedical Engineering* (3), 165–168 (1968)
8. Bhavasar, R., Sun, Y., Helian, N., Davey, N., Mayor, D., Steffert, T.: The correlation between eeg signals as measured in different positions on scalp varying with distance. *Procedia computer science* **123**, 92–97 (2018)
9. Cadzow, J.A.: Spectral estimation: An overdetermined rational model equation approach. *Proceedings of the IEEE* **70**(9), 907–939 (1982)
10. Carter, G., Knapp, C.: Coherence and its estimation via the partitioned modified chirp-z transform. *IEEE Transactions on Acoustics, Speech, and Signal Processing* **23**(3), 257–264 (1975)
11. Carter, G.C.: Coherence and time delay estimation. *Proceedings of the IEEE* **75**(2), 236–255 (1987)
12. Cohen, L.: Time-frequency distributions-a review. *Proceedings of the IEEE* **77**(7), 941–981 (1989)
13. Cohen, L.: The uncertainty principle in signal analysis. In: *Proceedings of IEEE-SP International Symposium on Time-Frequency and Time-Scale Analysis*. pp. 182–185. IEEE (1994)
14. Cohen, L.: The generalization of the wiener-khinchin theorem. In: *Proceedings of the 1998 IEEE International Conference on Acoustics, Speech and Signal Processing, ICASSP'98* (Cat. No. 98CH36181). vol. 3, pp. 1577–1580. IEEE (1998)
15. Dedovic, K., Renwick, R., Mahani, N.K., Engert, V., Lupien, S.J., Pruessner, J.C.: The montreal imaging stress task: using functional imaging to investigate the effects of perceiving and processing psychosocial stress in the human brain. *Journal of Psychiatry and Neuroscience* **30**(5), 319 (2005)
16. Deguire, F., Thébault-Dagher, F., Barlaam, F., Knoth, I.S., Lafontaine, M.P., Lupien, S., Lippé, S.: The relationship between acute stress and eeg repetition suppression in infants. *Psychoneuroendocrinology* (2019)
17. Fein, G., Raz, J., Brown, F.F., Merrin, E.L.: Common reference coherence data are confounded by power and phase effects. *Electroencephalography and clinical neurophysiology* **69**(6), 581–584 (1988)
18. Feinberg, I., Baker, T., Leder, R., March, J.: Response of delta (0-3 hz) eeg and eye movement density to a night with 100 minutes of sleep. *Sleep* **11**(5), 473–487 (1988)
19. Gardner, M.W., Dorling, S.: Artificial neural networks (the multilayer perceptron)—a review of applications in the atmospheric sciences. *Atmospheric environment* **32**(14-15), 2627–2636 (1998)
20. Gibson, G.J., Cowan, C.F.: On the decision regions of multilayer perceptrons. *Proceedings of the IEEE* **78**(10), 1590–1594 (1990)
21. Golden, C.J., Freshwater, S.M.: Stroop color and word test (1978)
22. Hagemann, D., Naumann, E.: The effects of ocular artifacts on (lateralized) broadband power in the eeg. *Clinical Neurophysiology* **112**(2), 215–231 (2001)

Stress coherence, spectrum and classification

23. Hayes, M.H.: Statistical digital signal processing and modeling. John Wiley & Sons (2009)
24. Haykin, S.: Neural networks: a comprehensive foundation. Prentice Hall PTR (1994)
25. Haykin, S.: A comprehensive foundation: Neural networks (1999)
26. Hazarika, N., Chen, J.Z., Tsoi, A.C., Sergejew, A.: Classification of eeg signals using the wavelet transform. *Signal processing* **59**(1), 61–72 (1997)
27. Hou, X., Liu, Y., Sourina, O., Tan, Y.R.E., Wang, L., Mueller-Wittig, W.: Eeg based stress monitoring. In: 2015 IEEE International Conference on Systems, Man, and Cybernetics. pp. 3110–3115. IEEE (2015)
28. Jones, E., Oliphant, T., Peterson, P., et al.: SciPy: Open source scientific tools for Python (2001–), <http://www.scipy.org/>, [Online; accessed]
29. Kay, S.M., Marple, S.L.: Spectrum analysis—a modern perspective. *Proceedings of the IEEE* **69**(11), 1380–1419 (1981)
30. Kingma, D.P., Ba, J.: Adam: A method for stochastic optimization. *arXiv preprint arXiv:1412.6980* (2014)
31. Klem, G.H., Lüders, H.O., Jasper, H., Elger, C., et al.: The ten-twenty electrode system of the international federation. *Electroencephalogr Clin Neurophysiol* **52**(3), 3–6 (1999)
32. Lin, D., Sun, L., Toh, K.A., Zhang, J.B., Lin, Z.: Biomedical image classification based on a cascade of an svm with a reject option and subspace analysis. *Computers in biology and medicine* **96**, 128–140 (2018)
33. Marosi, E., Harmony, T., Sánchez, L., Becker, J., Bernal, J., Reyes, A., de León, A.E.D., Rodríguez, M., Fernández, T.: Maturation of the coherence of eeg activity in normal and learning-disabled children. *Electroencephalography and clinical Neurophysiology* **83**(6), 350–357 (1992)
34. Mathews, J., Breakall, J., Karawas, G.: The discrete prolate spheroidal filter as a digital signal processing tool. *IEEE transactions on acoustics, speech, and signal processing* **33**(6), 1471–1478 (1985)
35. Modarres, M.H., Opel, R.A., Weymann, K.B., Lim, M.M.: Strong correlation of novel sleep electroencephalography coherence markers with diagnosis and severity of posttraumatic stress disorder. *Scientific reports* **9**(1), 4247 (2019)
36. Oppenheim, A.V.: Discrete-time signal processing. Pearson Education India (1999)
37. Pal, S.K., Mitra, S.: Multilayer perceptron, fuzzy sets, and classification. *IEEE Transactions on neural networks* **3**(5), 683–697 (1992)
38. Pedregosa, F., Varoquaux, G., Gramfort, A., Michel, V., Thirion, B., Grisel, O., Blondel, M., Prettenhofer, P., Weiss, R., Dubourg, V., et al.: Scikit-learn: Machine learning in python. *Journal of machine learning research* **12**(Oct), 2825–2830 (2011)
39. Rangaswamy, M., Porjesz, B., Chorlian, D.B., Wang, K., Jones, K.A., Bauer, L.O., Rohrbaugh, J., O'connor, S.J., Kuperman, S., Reich, T., et al.: Beta power in the eeg of alcoholics. *Biological psychiatry* **52**(8), 831–842 (2002)
40. Rappelsberger, P., Petsche, H.: Probability mapping: power and coherence analyses of cognitive processes. *Brain topography* **1**(1), 46–54 (1988)
41. Sandner, M., Lois, G., Wessa, M.: Characterizing the dynamic stress response on neuroendocrine and neural network level. *Psychoneuroendocrinology* **83**, 14 (2017)
42. Sasaki, K., Tsujimoto, T., Nishikawa, S., Nishitani, N., Ishihara, T.: Frontal mental theta wave recorded simultaneously with magnetoencephalography and electroencephalography. *Neuroscience research* **26**(1), 79–81 (1996)
43. Schacter, D.L.: Eeg theta waves and psychological phenomena: A review and analysis. *Biological psychology* **5**(1), 47–82 (1977)

M. C. Pedrino et al.

44. Schürmann, M., Başar, E.: Functional aspects of alpha oscillations in the eeg. *International Journal of Psychophysiology* **39**(2-3), 151–158 (2001)
45. Sejdić, E., Djurović, I., Jiang, J.: Time–frequency feature representation using energy concentration: An overview of recent advances. *Digital signal processing* **19**(1), 153–183 (2009)
46. Seo, S.H., Lee, J.T.: Stress and eeg. In: *Convergence and hybrid information technologies*. IntechOpen (2010)
47. Shaw, J., O'Connor, K., Ongley, C.: Eeg coherence as a measure of cerebral functional organization. In: *Architectonics of the cerebral cortex*, pp. 245–255. Raven Press New York (1978)
48. Srinivasan, R., Winter, W.R., Ding, J., Nunez, P.L.: Eeg and meg coherence: measures of functional connectivity at distinct spatial scales of neocortical dynamics. *Journal of neuroscience methods* **166**(1), 41–52 (2007)
49. Stoica, P., Moses, R.L., et al.: *Spectral analysis of signals* (2005)
50. Stroop, J.R.: Studies of interference in serial verbal reactions. *Journal of experimental psychology* **18**(6), 643 (1935)
51. Subasi, A.: Eeg signal classification using wavelet feature extraction and a mixture of expert model. *Expert Systems with Applications* **32**(4), 1084–1093 (2007)
52. Teplan, M., et al.: Fundamentals of eeg measurement. *Measurement science review* **2**(2), 1–11 (2002)
53. Thatcher, R.W., North, D., Biver, C.: Eeg and intelligence: relations between eeg coherence, eeg phase delay and power. *Clinical neurophysiology* **116**(9), 2129–2141 (2005)
54. Übeyli, E.D.: Combined neural network model employing wavelet coefficients for eeg signals classification. *Digital Signal Processing* **19**(2), 297–308 (2009)
55. Übeyli, E.D.: Decision support systems for time-varying biomedical signals: Eeg signals classification. *Expert Systems with Applications* **36**(2), 2275–2284 (2009)
56. Warner, S.: Cheat sheet for neurofeedback. Website Article, January (2013)
57. Welch, P.: The use of fast fourier transform for the estimation of power spectra: a method based on time averaging over short, modified periodograms. *IEEE Transactions on audio and electroacoustics* **15**(2), 70–73 (1967)
58. Whitton, J.L., Lue, F., Moldofsky, H.: A spectral method for removing eye movement artifacts from the eeg. *Electroencephalography and clinical neurophysiology* **44**(6), 735–741 (1978)
59. Xu, Y., Haykin, S., Racine, R.J.: Multiple window time-frequency distribution and coherence of eeg using slepian sequences and hermite functions. *IEEE Transactions on Biomedical Engineering* **46**(7), 861–866 (1999)